

Andre Palmer
Jingyuan Xu
Denis Wirtz

High-frequency viscoelasticity of crosslinked actin filament networks measured by diffusing wave spectroscopy

Received: 20 January 1998
Accepted: 12 February 1998

Abstract We study the short-time relaxation dynamics of crosslinked and uncrosslinked networks of semi-flexible polymers using diffusing wave spectroscopy (DWS). The networks consist of concentrated solutions of actin filaments, cross-linked with increasing amounts of α -actinin. Actin filaments (F-actin) are long semi-flexible polymers with a contour length 1–100 μm and a persistence length of 5–15 μm ; α -actinin is a small 200 kDa homodimer with two actin-binding sites. Using the large bandwidth of DWS, we measure the mean-square-displacement of 0.96 μm diameter microspheres imbedded in the polymer network, from which we extract the frequency-dependent viscoelastic moduli via a generalized Langevin equation. DWS measurements yield, in a single measurement, viscoelastic moduli at frequencies up to

10⁵ Hz, almost three decades higher in frequency than probed by conventional mechanical rheology. Our measurements show that the magnitude of the small-frequency plateau modulus of F-actin is greatly enhanced in the presence of α -actinin, and that the frequency dependence of the viscoelastic moduli is much stronger at intermediate frequencies. However, the frequency-dependence of loss and storage moduli become similar for both crosslinked and uncrosslinked networks at large frequencies, $G'(\omega) \propto G''(\omega) \propto \omega^{0.75 \pm 0.08}$. This high-frequency behavior is due to the small-amplitude, large-frequency lateral fluctuations of actin filaments between entanglements.

Key words Actin – α -actinin – diffusing wave spectroscopy – semi flexible polymer

A. Palmer · J. Xu · D. Wirtz (✉)
Department of Chemical Engineering
The Johns Hopkins University
3400 North Charles St.
Baltimore, MD 21218
USA
E-mail: wirtz@jhu.edu

Introduction

The short-time dynamics of polymers in entangled polymer solutions has long been the subject of research in theoretical polymer physics (Rouse, 1953; Zimm, 1954; Doi and Edwards, 1989). However, the limited bandwidth of current mechanical rheometers and spectroscopic techniques such as fluorescence recovery after photobleaching (FRAP) and forced-Rayleigh scattering (FRS) has not allowed one to test these theories directly. One of the few approaches to extract high-frequency dynamical properties of polymer systems such as loss and storage moduli

has involved in using the time-temperature superposition (Ferry, 1980). By decreasing the temperature of a polymer melt or solution, both the terminal relaxation time and entanglement time describing the onset of entanglements can be conveniently increased and the relaxation times become measurable by rheometric techniques. However, polymer blends and solutions may undergo phase transitions upon a temperature change. The proximity to a phase boundary line can dramatically affect the dynamics of relaxation since large length scale correlations dominate the physics of relaxation in near-critical polymer systems, not the small length scale mo-

tion of individual polymers. Furthermore, many polymers such as protein macromolecular assemblies degrade rapidly upon temperature changes, therefore the time-temperature superposition cannot be conducted unambiguously with these systems.

The advent of diffusing wave spectroscopy (Weitz and Pine, 1993) and particle-tracking microrheology (Mason et al., 1997; Mason et al., 1997; Gittes et al., 1997; Schnurr et al., 1997) have allowed to monitor the high-frequency viscoelastic moduli of polymer gels and entangled solutions. These techniques probe viscoelastic moduli over an extended frequency range in a single experiment at a fixed temperature. These techniques monitor the thermally excited motion of microspheres imbedded in a polymer solution. Using a Langevin description of the motion of a microsphere in a viscoelastic fluid, one can extract viscoelastic moduli (Mason and Weitz, 1995; Mason et al., 1997) and creep compliance (this work) from the measured mean square displacement. Using DWS, the mean square displacement of the probing microsphere can be monitored with nanosecond resolution; using particle-tracking microrheology, the mean square displacement can be monitored with sub-millisecond resolution. As a result, the mechanical properties of polymer networks and solutions can be measured at frequencies as high as 10^6 rad/s, almost three orders of magnitude larger than probed by conventional mechanical rheometers. From these high-frequency measurements, we can gain a new insight into the mechanism of early dynamics of stress relaxation in entangled networks and an understanding of the type of local macromolecular motion which produces stress relaxation at short times. This new insight allows us to test current models of polymer motion at short length scales and short time scales.

The polymer motion inside an entangled polymer solution at small times, or equivalently at large frequencies, is typically described as that of a free polymer. Therefore in the case of flexible polymers, Zimm and Rouse models of dynamics in dilute solutions have been used to describe the relaxation at time scales smaller than the entanglement time τ_e (Rouse, 1953; Zimm, 1956). At times longer than τ_e , the effects of entanglements become important and the polymer motion is assumed to be confined inside a tube; reptation dominates the mechanism of relaxation (Doi and Edwards, 1989). The decoupling between reptation at long times and Rouse-like dynamics at short times has not been formally tested with non-invasive techniques in entangled polymers (Doi and Edwards, 1989). The limited bandwidth of mechanical rheometers has also prevented a systematic study of the effect of backbone rigidity and degree of crosslinking on the early dynamics of relaxation in polymer solutions.

In this paper, we study the effect of transient crosslinking on the short-time motion of actin filaments in a

“tightly entangled” network (Morse, 1997). Actin filaments are long semi-flexible polymers (Alberts et al., 1994), with an extremely long persistence length $l_p \approx 5\text{--}15\ \mu\text{m}$ compared to their diameter $d \approx 1\ \mu\text{m}$ (Gittes et al., 1993; Isambert et al., 1995). At large concentrations, actin filaments form a “tightly entangled network” because the persistence length of F-actin is much larger than the entanglement length l_e . The entanglement length $l_e \approx 1\ \mu\text{m}$ can be defined as the distance between collisions of a polymer with the confining walls of the tube (Morse, 1997). The tightly entangled regime, which corresponds to contour length densities $\rho \gg 1/l_p^2 \approx 4.4 \cdot 10^{-3}\ \mu\text{m}^{-2}$, is intermediate between the loosely entangled regime and the nematic regime. According to the Onsager criteria, the nematic regime corresponds to concentrations $\rho > \rho_{nem} \approx 10/Ld \approx 150\ \mu\text{m}^{-2}$. The loosely entangled regime corresponds to concentrations large enough that polymer are entangled, but smaller than $1/l_p^2$. In this regime, the entanglement length is much larger than the persistence length ($l_e \gg l_p$). Most semi-flexible polymers are not rigid enough and long enough to display this intermediate regime, which is widest when the ratio l_p/d is the largest. Therefore, filamentous actin constitutes one of the few polymers which allow us to probe the intermediate “tightly-entangled” regime of semi-flexible polymers.

One can envision that, at time scales smaller than a characteristic time τ_e , the fast small length scale bending modes of wavelength $\lambda < l_e$ dominate the (transverse) motion of the semi-flexible polymer. One can further assume that, when the polymer is not crosslinked and at time scales larger than τ_e , the motion of the semi-flexible polymer becomes hindered by the tube formed by the surrounding polymers and can only relax via reptation. When the polymer is crosslinked, reptation becomes progressively prohibited and only the short-time relaxation of subsections of entanglements is allowed.

As a dynamical crosslinker of actin, we use α -actinin, a small 200 kDa protein with two actin-binding sites. In the tightly entanglement regime for which $l_p \gg l_e$, actin filaments are rigid between entanglements, therefore little contour length fluctuation relaxes longitudinally. Therefore, in the case of permanent crosslinks and for mechanical rheometers which have a limited bandwidth, loss and storage moduli are featureless, i.e. $G'(\omega)$ and $G''(\omega)$ are independent of frequency. In the present case, the crosslinking protein α -actinin has a finite lifetime of binding to actin; hence crosslinking of α -actinin to F-actin is transient. Our new DWS measurements show that the magnitude of the small-frequency plateau modulus of actin networks is greatly enhanced in the presence of α -actinin, and that the frequency dependence of the viscoelastic moduli is much stronger at intermediate frequencies. The frequency-dependence of loss and storage moduli become

similar for both crosslinked and uncrosslinked networks at large frequencies, $G'(\omega) \propto G''(\omega) \propto \omega^{0.75 \pm 0.08}$.

Methods and systems

Preparation of actin and α -actinin

Actin was extracted from rabbit skeletal muscle acetone powder by the method of Spudich and Watt (1971). The resulting actin was then gel filtered on Sephacryl S-300 HR instead of Sephadex G-150 (MacLean-Fletcher and Pollard, 1980). The purified actin was stored as Ca^{2+} -actin in continuous dialysis at 4 °C against daily changed buffer G (0.2 mM ATP, 0.5 mM DTT, 0.1 mM CaCl_2 , 1 mM NaAzide, and 2 mM tris-Cl, pH 8.0). The final actin concentration was determined by ultraviolet absorbance at 290 nm, using an extinction coefficient of $2.66 \times 10^4 \text{ M}^{-1} \text{ cm}^{-1}$, and a cell path length of 1 cm. Actin filaments were generated by adding 0.1 volume of 10-x KME (500 mM KCl, 10 mM MgCl_2 , 10 mM EGTA, 100 mM imidazole, pH 7.0) polymerizing salt buffer solution to 0.9 volume of G-actin in buffer G. The actin used for all experiments came from the last fraction of the actin peak obtained by one gel filtration. Alpha-actinin from *Acanthamoeba Castellani* is purified as described in Wachstock et al. (1993, 1994) and was a gift of Drs. Mullins, Kelleher, and Pollard. This α -actinin was further gel-filtrated on Sephacryl S-300 HR in equilibrium with Buffer G. SDS electrophoresis showed that the purity of the α -actinin was greater than 90%.

Diffusing wave spectroscopy

The beam from an Ar^+ -ion laser operating in the single-line-frequency mode at a wavelength of 514 nm is focused and incident upon a flat scattering cell which contains the polymerized actin solution and spherical optical probes. The light multiply scattered from the solution is collected by two photomultiplier tubes (PMT) via a single-mode optical fiber with a collimator lens of very narrow angle of acceptance at its front end and a beamsplitter at its back end. The outputs of the PMTs are directed to a correlator working in the pseudo cross-correlation mode to generate the autocorrelation function $g_2(t)-1$ from which quiescent rheological properties of the actin solutions can be calculated. The mean square displacement of the probing spheres is extracted from $g_2(t)-1$ measurements via a root-search algorithm following classical techniques (Weitz and Pine, 1993).

Viscoelastic moduli of crosslinked and uncrosslinked actin filament networks are calculated from measured mean-square displacements via a generalized Langevin

equation of diffusion of a microsphere in a viscoelastic fluid (Mason and Weitz, 1995). Briefly, the local viscoelastic modulus of a fluid and the mean square displacement of a microsphere suspended in that fluid are related via³

$$\tilde{G}(s) = \frac{s}{6\pi a} \left[\frac{6k_B T}{s^2 \langle \Delta \tilde{r}^2(s) \rangle} - ms \right] \approx \frac{k_B T}{\pi a s \langle \Delta \tilde{r}^2(s) \rangle}, \quad (1)$$

where k_B is Boltzmann's constant, T is the temperature of the sample, a is the radius of the microsphere, m , is its mass, s is the Laplace frequency, and $\tilde{\cdot}$ represents the unilateral Laplace transformation defined as $\tilde{X}(s) \equiv L[X(t)] \equiv \int_0^\infty X(t) \exp(-st) dt$. Equation (1) relates the unilateral Laplace transform of the stress relaxation modulus $G_r(t)$, $\tilde{G}(s) \equiv s\tilde{G}_r(s)$, to the Laplace transform of the mean-square displacement $\langle \Delta r^2(t) \rangle$. In Eq. (1), the inertia term (the second term in the brackets) is neglected because it corresponds to very high frequencies, of the order 10^6 Hz. The knowledge of $\tilde{G}(s)$ is typically sufficient to characterize the rheological behavior of a polymer solution. However, in order to present our optical measurements in a more familiar fashion, we use the analytic continuation between the real function $\tilde{G}(s)$ and the complex function $G^*(\omega) \equiv G'(\omega) + iG''(\omega)$. We extract storage and loss moduli by replacing s by $i\omega$ in $\tilde{G}(s)$ and by extracting real and imaginary parts from the resulting imaginary function $\tilde{G}(s = i\omega)$, respectively. Equation (1) yields the correct results for the extreme cases of a purely viscous liquid and purely elastic solid. For a viscous liquid, $\langle \Delta \tilde{r}^2(s) \rangle = 6D/s^2 = k_B T / \pi \eta a s^2$ and $\tilde{G}(s) = \eta s$ where η is the constant viscosity of the liquid; therefore $G'(\omega) = \eta$ and $G''(\omega) = \eta_s \omega$. Instead, for an elastic solid, $\langle \Delta \tilde{r}^2(s) \rangle = r_0^2$ and $\tilde{G}(s) = G_0 = k_B T / \pi a r_0^2$ where G_0 is the elastic modulus; therefore, $G'(\omega) = G_0$ and $G''(\omega) = 0$. A viscoelastic fluid such as an actin gel has both non-vanishing loss and storage moduli.

Actin is polymerized in situ for 12 h before measurement by loading the scattering cell with a solution of monomeric actin mixed with the polymerizing salt solution and a dilute suspension of monodisperse latex microspheres (Duke Scientific Corp.) of radius 0.48 μm at a volume fraction of 0.01. The scattering cell is then immediately tightly capped. We verified by both time-resolved static light scattering and time-resolved mechanical rheology that G-actin was fully polymerized into F-actin at all concentrations presented in this paper before 24 h. Using static light scattering, we verified that more than 99% of the scattering intensity in the transmission geometry was due to the microspheres, less than 1% due to the actin filament network itself. We also verified using mechanical rheology that the added latex beads did not affect the rheology of polymerized actin, representing less than 5% of the magnitude of $G'(\omega)$ and $G''(\omega)$ at all actin concentrations

used in this paper. All DWS measurements are conducted at a temperature of $T=23^\circ\text{C}$.

Results and discussion

Diffusion of a microsphere in a crosslinked actin network

The frequency-dependent viscoelastic moduli of crosslinked and uncrosslinked actin filament networks are deduced from the time-dependent mean-square displacements of $0.96\ \mu\text{m}$ diameter microspheres imbedded in the F-actin solutions. Measurements of the mean-square displacements and associated diffusion coefficients in the temporal domain provide us with a new physical insight into the dynamics of relaxation of crosslinked and uncrosslinked actin gels complementary to the insight gained from rheological measurements. The measurements of mean square displacements, unlike the viscoelastic moduli calculated using Eq. (1), are model-independent.

Mean square displacement

The mean square displacement $\langle\Delta r^2(t)\rangle$ is extracted from the measured autocorrelation function $g_2(t)-1$ of the light multiple scattered by the microspheres mixed with the actin solution. Using an efficient custom root-searching program, we calculate $\langle\Delta r^2(t)\rangle$ with nanosecond temporal resolution and nanometer spatial resolution. Figure 1 shows the correlation function $g_2(t)-1$ for

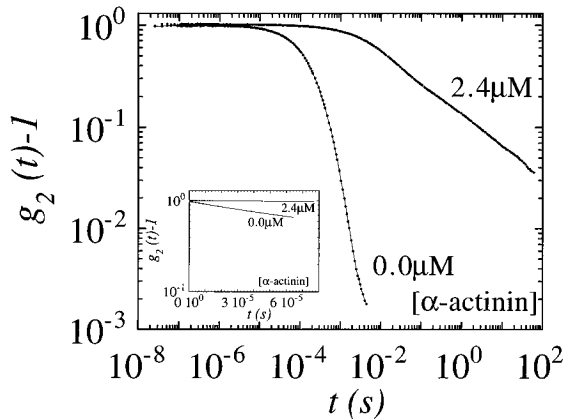


Fig. 1 Autocorrelation function of the light intensity multiply scattered by the $0.96\ \mu\text{m}$ diameter microspheres imbedded in a $24\ \mu\text{M}$ actin network in the presence or in the absence of crosslinkers. The relaxation of the correlation function is observed to be retarded by the presence of crosslinkers. The mean square displacement of the probing microspheres is extracted from these measurements and shown in Fig. 3

concentrated solutions of pure actin filaments and concentrated solutions of actin filaments crosslinked with increasing amounts of crosslinkers. We observe that the presence of crosslinkers in F-actin solutions retard the relaxation of the intensity autocorrelation function. This effect is accentuated for increasing amounts of crosslinkers. At short times, the correlation function undergoes (approximately) exponential decay for both crosslinked and uncrosslinked actin networks, as shown in the inset of Fig. 1, which shows $g_2(t)-1$ decreasing linearly with time in a log-linear plot.

Figure 2 displays the mean square displacement calculated from the measurements of $g_2(t)-1$. For pure actin and at early times, we observe that the mean square displacement varies with time as $\langle\Delta r^2(t)\rangle \propto t^a$ with $a=0.75\pm 0.05$. Therefore even at the earliest times probed by DWS, $t < 10^{-5}\ \text{s}$, we observe that the motion of $0.96\ \mu\text{m}$ microspheres in actin filament networks is sub-diffusive with an exponent a smaller than 1. An exponent $a=1$ would correspond to the free Brownian diffusion of the microspheres in the suspending solution. For actin crosslinked with α -actinin, we observe that while the displacements of the same microspheres are much smaller in amplitude, the temporal dependence of the mean square displacement is similar to that observed with uncrosslinked actin networks. For crosslinked actin networks, the exponent representing the variation of $\langle\Delta r^2(t)\rangle$ with time seems to decrease slightly from $a=0.75$ to $a=0.68$ for increasing amounts of crosslinkers. This slight decrease of the exponent can be due to the fact that the fitting of the mean square

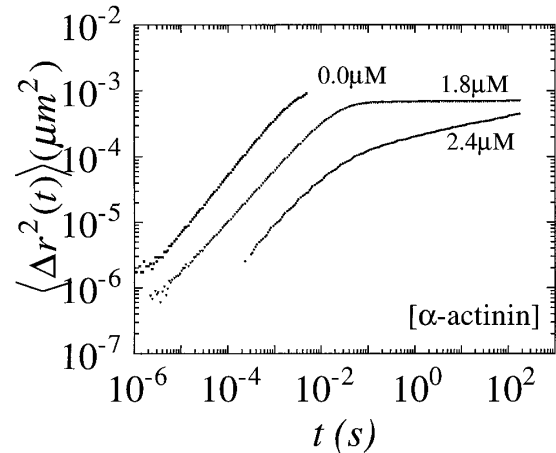


Fig. 2 Mean square displacement of $0.96\ \mu\text{m}$ microspheres of pure actin filament networks. At short-times $\langle\Delta r^2(t)\rangle \propto t^{0.75}$. At long times, the microspheres' motion becomes hindered by the tight entangled network. Mean square displacement of the same microspheres in the same actin network, but crosslinked with increasing amounts of crosslinking proteins, α -actinin. The onset of the large-time plateau occurs earlier than for uncrosslinked networks. However, the time-dependence of the mean square displacement is identical to that observed in uncrosslinked actin networks

displacement curves is not obtained in the power-law regime. As shown in Fig. 2, the power law regime occurs past a characteristic time, which decreases with increasing concentration of crosslinkers.

The thermally excited motion of $0.96\ \mu\text{m}$ microspheres in a $24\ \mu\text{M}$ actin solution is sub-diffusive because its size is much smaller than the mesh size of the network. At short times and due to its size, the probing microspheres cannot percolate through the network; instead, they are elastically trapped by the mesh. As shown by Fig. 2, the magnitude of the displacements is always much smaller than the diameter of the microsphere and smaller than the mesh size of the actin network. Also, the relaxation time of the individual actin filaments is huge ($\tau_D \approx 10^3\text{--}10^4\ \text{s}$). Hence, over the probed temporal range, the individual filaments surrounding the microspheres do not fully disengage from their tube. A microrheological signature of full relaxation is a re-increase of $\langle \Delta r^2(t) \rangle$ after the plateau at intermediate times. Our mean square displacements are not conducted over long enough periods of time to capture this final relaxation.

It is interesting to invoke the proportionality between the mean square displacement and the shear creep compliance $J(t)$,

$$J(t) = \frac{\pi a}{k_B T} \langle \Delta r^2(t) \rangle \quad (2)$$

This relation is demonstrated in the appendix. Equation (1) directly relates the local displacement of a microsphere imbedded in a polymer network to the local mechanical properties of that network. The shear creep compliance of a network corresponds to the deformation of that network normalized by the applied stress. Here, the force generated by the thermal motion of the microsphere in the surrounding network, or equivalently generated by the thermal motion of the network on the probing microsphere, is small since it is of thermal origin and is of the order $k_B T/a$. If the fluid were purely viscous, $J(t) = t/\eta \propto t$; if the fluid were purely solid-like $J(t) = J_0 \propto t^0$. Therefore, an exponent $a \approx 0.75$ indicates that an actin network dissipates energy more than it stores energy at short time scales. The inset in Fig. 2 shows the creep compliance for actin networks in the presence and in the absence of crosslinkers. Our DWS measurements suggest that while the creep compliance in an uncrosslinked network is much smaller than in an uncrosslinked network, the rate of increase of the creep compliance is similar for crosslinked and uncrosslinked actin networks at short times.

At longer times, the displacement of the microsphere in the uncrosslinked actin network is slowed. The microsphere becomes progressively trapped by the tight, elastic actin network. The origin of this trapping is entropic as verified by analytical centrifugation and gel electrophoresis (not shown here), which showed no

chemical binding of the microsphere with actin. At long times, the displacement of the same microsphere in a crosslinked network remains smaller than for an uncrosslinked actin network. However, the rate of change of the mean square displacement is unexpectedly stronger for increasing amounts of crosslinkers. We shall see below that this effect is due to the finite lifetime of binding of α -actinin to F-actin. This indicates that the mechanism of stress relaxation becomes similar for crosslinked and uncrosslinked actin networks at short times.

Diffusion coefficient

The displacement of a microsphere in an entangled actin network can be further analyzed by extracting the time-dependent diffusion coefficient from the mean square displacement measurements. We define the time-dependent diffusion coefficient as

$$D(t) \equiv \langle \Delta r^2(t) \rangle / 6t \quad (3)$$

Figure 3 displays $D(t)$ for various actin concentration and α -actinin concentrations. We find that the diffusion coefficient of the microsphere in the actin network is smaller than the bare diffusion coefficient of the same microsphere in the same buffer solution viscous fluid, given by $D_0 = k_B T / 6\pi\eta_s a \approx 0.45\ \mu\text{m}^2/\text{s}$, where $\eta_s \approx 1\ \text{cP}$ is the ‘‘microviscosity’’ of the buffer solution. Of course, since the microsphere’s motion of subdiffusive, the tracer diffusion coefficient becomes rapidly much smaller than D_0 at times $t > 10^{-5}\ \text{s}$. Figure 3 shows that, as expected from the data in Fig. 2, the diffusion coefficient of the microsphere is always smaller for a crosslinked actin network, due to the hindered diffusion of actin filaments in the presence of crosslinkers. Figure 3 also shows that the diffusion of a $0.96\ \mu\text{m}$ microsphere in a crosslinked or uncrosslinked actin network cannot be represented by the constant Brownian diffusion coefficient in a fluid of effective macroscopic viscosity $\eta \approx 1\ \text{P}$, the macroscopic viscosity of $24\ \mu\text{M}$ actin solution. The diffusion coefficient would be a constant equal to $D = k_B T / 6\pi\eta a \approx 4.5 \cdot 10^{-3}\ \mu\text{m}^2/\text{s}$. The diffusion coefficient of a $0.96\ \mu\text{m}$ microsphere depends strongly on time, which reflects not only the viscoelastic nature of the fluid, but also its multi-component structure.

Small frequency viscoelastic moduli

The mean square displacement of a microsphere in a polymer network is also directly related to the bulk viscoelastic moduli of that network. These moduli include the frequency-dependent storage modulus $G'(\omega)$, the loss modulus $G''(\omega)$, and amplitude of the viscoelastic

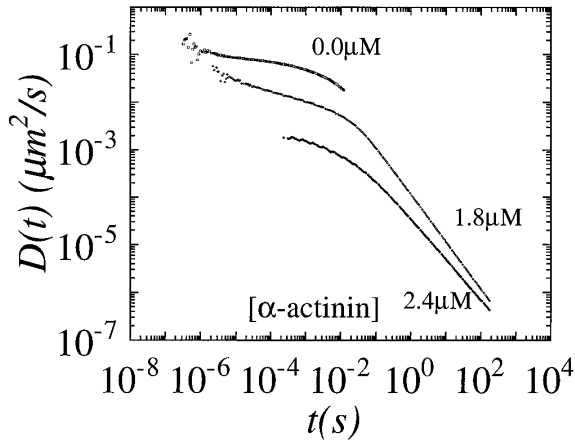


Fig. 3 Time-dependent diffusion coefficient, $D(t) \equiv \langle \Delta r^2(t) \rangle / 6t$, of microspheres imbedded in crosslinked and uncrosslinked actin networks for increasing α -actinin concentration. The microsphere's radius a is much larger than the actin network mesh size $a \gg \xi \approx 0.15 \mu\text{m}$ for $c=24 \mu\text{M}$. At times as short as 10^{-6} s, the transport of the microsphere is sub-diffusive. The corresponding diffusion coefficient is smaller than that of the same microsphere in water. Same conditions as in Fig. 2

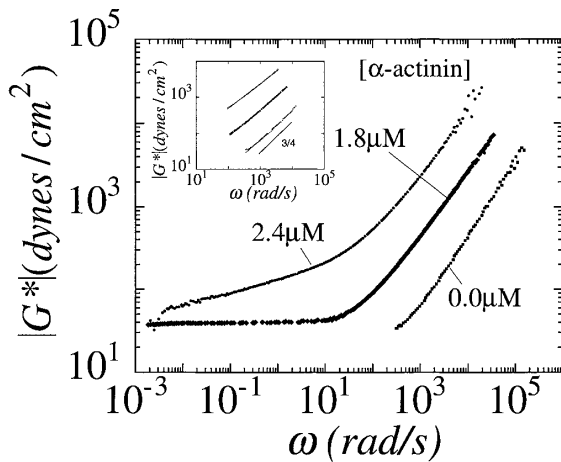


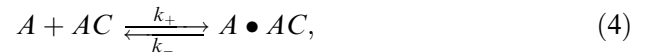
Fig. 4 Magnitude of the frequency dependence viscoelastic modulus of actin networks, crosslinked with increasing amounts of α -actinin measured by DWS. At large frequencies, $|G^*(\omega)| \propto \omega^{0.75}$ for the low-concentration isotropic phase, the large-concentration nematic phase, and the crosslinked forms of actin networks. This exponent reflects the finite rigidity of actin filaments and is due to the high-frequency lateral fluctuations of the actin filaments between entanglements

modulus $|G^*(\omega)| = \sqrt{G'^2(\omega) + G''^2(\omega)}$. As detailed in other papers, the transformation from mean square displacements to viscoelastic moduli can be achieved via two different, but related schemes (Mason and Weitz, 1995; Mason et al., 1997; Gittes et al., 1997).

Figure 4 shows DWS measurements of the amplitude of the viscoelastic modulus $|G^*(\omega)|$ of an actin network in the presence and in the absence of crosslinking pro-

teins calculated from the measured mean square displacements in Fig. 2. One of the most striking differences between crosslinked and uncrosslinked actin networks is the frequency dependence of $|G^*(\omega)|$. In the absence of crosslinkers, the viscoelastic modulus of an F-actin network is relatively independent of frequency at frequencies up to 100 rad/s. In the presence of crosslinkers, the viscoelastic modulus becomes a strong function of frequency at frequencies as low as 10^{-3} rad/s. These optical measurements are in agreement with rheological measurements by Wachstock et al. (1993, 1994), at least at small frequencies. The viscoelastic behavior of crosslinked and uncrosslinked actin networks is similar at very small and very large frequencies. As suggested by Sato et al. (1989), the strong dependence of the viscoelastic moduli with frequency at intermediate frequencies can be attributed to the dynamics of attachment of α -actinin with F-actin.

One can describe the dynamic attachment of *Acanthamoeba* α -actinin (AC) with actin (A) as an association reaction of the type (Wachstock et al., 1993, 1994; Tempel et al., 1996).



where k_+ and k_- are the association and dissociation rates, respectively. Wachstock et al. (1993) measured $k_+ = 1 \mu\text{M}^{-1} \text{s}^{-1}$, $k_- = 5.2 \text{s}^{-1}$, and $K_d = k_-/k_+ = 0.19 \mu\text{M}$. Therefore, the lifetime of a binding event between α -actinin and F-actin is $1/k_- = 0.19$ s. Unlike the more familiar case of chemical gels, for which crosslinks are permanent, the lifetime of binding of α -actinin to F-actin is relatively short. As a result, viscoelastic moduli are frequency dependent as easily observed within the frequency range probed by optical rheometry and mechanical rheometry. At very small frequencies or long time scales, most crosslinkers are statistically detached from the actin polymers and the crosslinked actin network behaves as if it were uncrosslinked. This interpretation is supported by Fig. 4: the magnitude of $|G^*(\omega)|$ becomes similar for crosslinked and uncrosslinked actin networks. At larger frequencies or shorter time scales, most crosslinkers are attached to the filaments, which slows down the relaxation of the stress at short times, or equivalently, increases the viscoelastic moduli at large frequencies. However, as shown by Fig. 4, we do not observe a sharp increase of the viscoelastic modulus at the frequency corresponding to the inverse of the lifetime of the crosslink. The increase of $|G^*(\omega)|$ with frequency is observed to occur even at frequencies much smaller than k_- . This result suggests that in order for the stress to relax in a crosslinked network, the crosslinks need to relax somewhat cooperatively, which decelerates the stress relaxation. Furthermore, $|G^*(\omega)|$ is observed to remain a strong function of frequency at frequencies much larger than k_- . By analogy with the

classical rheological behavior of chemical gels, which display a large elastic plateau over an extended frequency range, one could have expected a rather frequency-independent profile for $|G^*(\omega)|$ at frequencies $\omega > k_-$. At very large frequencies, $\omega \gg k_-$, the frequency dependence and the magnitude of $|G^*(\omega)|$ become similar again to the case of an uncrosslinked actin network. We shall further discuss the high-frequency regime below.

Note that these optical measurements have the important advantage over classical mechanical measurements in that they avoid possible shear-induced orientation of the network. As shown in a separate paper (Wirtz et al., 1998), the presence of crosslinkers can dramatically reduce the range of strain values for which one can measure the rheological properties of actin networks in the linear regime. In these papers, we studied the effect of strain in steady and oscillatory shear on the viscoelastic moduli of crosslinked and uncrosslinked networks. We observed that in the presence of crosslinkers, strains as small as 2% can generate strain-hardening. This strain hardening behavior subsists over a small strain range. Past a strain of 10%, crosslinked actin networks yield rapidly. Diffusing wave spectroscopy does not involve any forced shearing of the probed actin networks. Therefore, DWS measurements can effectively probe the rheology of crosslinked actin gels in the linear regime, which is difficult to achieve by classical mechanical rheometry.

High-frequency viscoelastic moduli

The extended frequency range probed by DWS allows us to probe the early dynamics of relaxation of crosslinked and uncrosslinked polymers in a network. The inset in Fig. 4, shows the viscoelastic modulus at frequencies $\omega > 10^3$ Hz. At those frequencies, the viscoelastic moduli of both crosslinked and uncrosslinked actin networks are observed to increase with similar effective power laws of frequency, $|G^*(\omega)| \propto \omega^a$ with $0.75 < a < 0.8$. However, as reflected by the time-dependence of the mean square displacement at short times, we observe a systematic decrease of the effective exponent from 0.80 to 0.75 when the ratio crosslinker concentration is decreased from 2.4 to 1.8 μM .

In this high frequency power law regime, the loss modulus dominates the elastic modulus, which is a consequence of the fact that $a > 1/2$. Indeed, the ratio between the loss modulus and the storage modulus is larger than once since $G''/G' = \tan(\alpha\pi/2)$ or $G'' \approx 2.41G'$, independently of frequency. This result can be contrasted to the more usual case of (smaller) synthetic flexible such as polystyrene in toluene and semi-flexible polymers such as PBLG in m-cresol for which $G' > G''$ even at the high frequencies probed by particle

tracking microrheology (Mason et al., 1997; Gittes et al., 1997; Schnurr et al., 1997) and DWS (Weitz and Pine, 1993). Of course, at extremely high frequencies, $\omega > 1$ MHz, the dissipation from the solvent dominates the rheology of actin filament networks since it grows with frequency as

$$|G^*| \approx G'' \approx \eta_\infty \omega, \quad (5)$$

where η_∞ is the high-frequency viscosity of the buffer solution. Our DWS measurements do not display the linear dependence predicted by Eq. (5), as shown in Figs. 4 and 5. Therefore, the viscoelastic properties of actin networks at the largest frequencies measured by DWS are dominated by the local dissipative motion of the actin filaments.

We can attempt to understand the dynamics of stress relaxation in crosslinked actin networks at intermediate and large frequencies by comparing the density of crosslinkers with the density of potential crosslinking points in the actin gel. For a 24 μM actin solution, the average density of overlaps is $\approx 1/\xi^3 \approx 300 \mu\text{m}^{-3}$, where $\xi \approx 0.15 \mu\text{m}$ is the average distance between overlapping actin filaments (i.e. the mesh size). Due to their small size and the presence of two F-actin binding sites, the only effective way that α -actinin molecules can bind to F-actin is to be located at a topological overlap between filaments. Therefore, if an α -actinin molecule is bound to one actin filament, after some time it will actively create an effective overlap with a second filament. The number of overlaps per chain is approximately $L/\xi \approx 140$, where $L \approx 20 \mu\text{m}$ is the average contour length of an actin filaments. L/ξ would represent the maximum number of available sites along an actin filament for crosslinking by α -actinin. Ignoring the finite lifetime of the crosslinker, for α -actinin concentrations between 1.8–2.4 μM , the average density of crosslinkers is $\approx 1.1\text{--}1.4 \cdot 10^3 \mu\text{m}^{-3}$. For a 24 μM actin solution, the contour length density of polymer is $\rho = c l_A N_A \approx 38.5 \mu\text{m}^{-2}$, where N_A is the Avogadro number and $l_A = 2.75 \text{ nm}$ is the curvilinear length of a G-actin monomer (Alberts et al., 1994). Hence, the curvilinear length between crosslinkers along each actin filament is about 0.026–0.036 μm . Therefore, 100% of polymer overlaps are associated with a crosslinker. This assumes that all α -actinin molecules crosslink actin filaments, which overestimates the number of α -actinin molecules attached to F-actin since crosslinks have a finite lifetime. Also, when α -actinin concentration becomes large, it has been observed that actin filaments do not form isotropic networks: actin filaments bundle (Wachstock et al. 1993, 1994).

At times much longer than the average lifetime of a crosslink, the number of α -actinin molecules that are bound is reduced and the effective number of overlaps associated with a crosslinker becomes smaller than 100%. Since fewer crosslinkers are bound, the dynamics

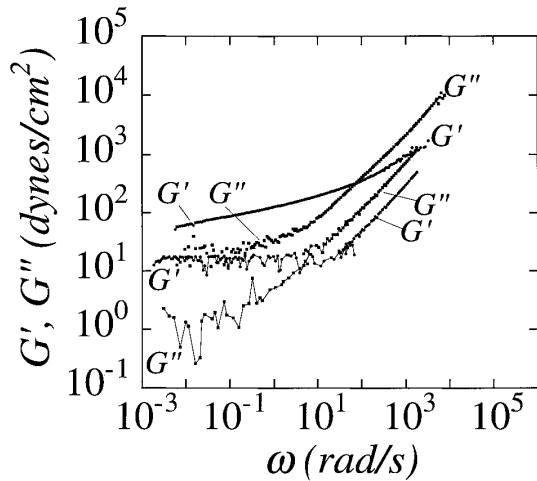


Fig. 5 Loss and storage moduli of actin networks, crosslinked with increasing amounts of *a*-actinin measured by DWS. We observe that the crossover frequency at which the loss modulus becomes larger than the elastic modulus is decreased for increasing crosslinker concentrations. We also observe that, for crosslinked actin networks, the elastic modulus is more frequency dependent at intermediate frequencies

of relaxation of crosslinked actin filaments becomes similar to the dynamics of relaxation in an uncrosslinked network at long time scales or large frequencies, as observed in Figs. 4 and 5. A similar interpretation of the data results if we remember that the mean square displacement of the probing microspheres is the normalized creep compliance of the network under stress. At time longer than the lifetime of crosslinking of *a*-actinin to F-actin, the deformation or creep of a strained actin network becomes relatively independent of the crosslinkers.

At intermediate times, the finite lifetime of binding of *a*-actinin becomes important. In an uncrosslinked actin network, the time at which effects of entanglements become important is of the order of $\tau_e \approx \zeta l_e^4 / k_B T l_p$, where ζ is the friction coefficient of actin filament per unit length. According to Morses' model (1997), for times $t \ll \tau_e$, the dynamics of relaxation is dominated by the bending modes or transverse fluctuations of actin at wavelengths smaller than the entanglement length. Since actin filaments are effectively rigid between entanglements ($l_p \gg (l_e, \zeta)$), then actin filaments cannot relax by contour length diffusion, unlike flexible polymers. The dynamics of stress relaxation in a semi-flexible polymer solution are dominated by the lateral motion of the filaments between entanglements. This motion becomes rapidly hindered for times $t > \tau_e$. The forces which prevent this small lateral motion generate a stress called the "tension" stress. In a crosslinked actin network, the nature of the dynamics of crosslinked actin networks should become similar to the dynamics of uncrosslinked networks. This reasoning holds as long as the distance

between crosslinkers does not become much smaller than the distance between overlaps and at short times.

The entanglement length, which is about $l_e \approx 0.5$ – $1.0 \mu\text{m}$, is larger than the average distance between overlaps saturated by a crosslinker. This might explain why effects of crosslinking become observable in viscoelastic spectra at high frequencies, i.e., the power-law behavior is quickly shortened by the presence of crosslinkers.

The early onset of crosslinking effects is also observed in Fig. 5, which displays the loss and storage moduli as a function of frequency for actin gels crosslinked with increasing amounts of *a*-actinin. At small *a*-actinin concentrations, the storage modulus is relatively flat at small frequencies, and increases as $G'(\omega) \propto \omega^{3/4}$ at large frequencies. At larger *a*-actinin concentrations, the storage modulus is a strong function of frequency and reaches a power-law behavior at large frequencies. Also the crossover frequency at which loss and storage moduli become equal, $G'(\omega) = G''(\omega)$, decreases for increasing *a*-actinin concentrations.

We recently showed that, in the absence of crosslinkers, the "curvature" stress, which stems from the slow reptation of actin in its tube, dominates the stress at small frequencies. At large frequencies and in the absence of crosslinkers, the stress is instead dominated by the tension stress, which is characterized by $G_{tens} \propto \omega^{3/4}$ (Schnurr et al., 1997). The tension stress originates from the restricted bending motion of actin filaments between entanglements. We also observe a $\omega^{3/4}$ dependence for G' and G'' at large frequencies in the presence of crosslinkers, which is the first evidence that the tension stress also dominates the stress for crosslinked actin networks at large frequencies. For crosslinked networks at small frequencies, one can suspect that, since reptation is greatly prohibited, the curvature stress is diminished. A direct clue for the absence of curvature stress in a crosslinked actin network is the steep frequency dependence of G' at small and intermediate frequencies. By contrast, G' reaches a true plateau modulus for uncrosslinked actin networks. This plateau modulus was shown to vary with concentration as $G'_p \propto c^{1.2 \pm 0.2}$ (Wirtz et al., 1997), which is characteristic of a curvature stress. We are currently studying the effect of actin concentration of the magnitude of G' and G'' over an extended frequency range for crosslinked actin networks. Since $G_{tens} \propto c^{2.25}$ as opposed to $G_{curve} \propto c^{1.4}$ (Morse, 1997), that study could help further identify the origin of the stress in a crosslinked actin network at small and large frequencies.

Summary and conclusions

We have presented DWS measurements of the short-time motion of semi-flexible polymers in a crosslinked solution of semi-flexible polymers. The system that we

studied consists of actin filament networks crosslinked with *Acanthamoeba a*-actinin, a small protein with two actin binding sites. Using the large bandwidth of diffusing wave spectroscopy, we measured the mean square displacement of small microspheres imbedded in crosslinked and uncrosslinked actin networks over an extended frequency range. From these mean square displacement measurements, we extracted the creep compliance and the viscoelastic moduli of the actin network. We observed that the scaling nature of crosslinked actin networks is similar to that of uncrosslinked networks both at extremely small and extremely large frequencies. At extremely small frequencies, which corresponds to time scales larger than the lifetime of a crosslinker, the motion of actin filaments is facilitated and resembles that of uncrosslinked actin filaments. However, the finite lifetime of crosslinking renders the viscoelastic moduli frequency dependent at intermediate frequencies. At very large frequencies, the modulus varies with frequency as $|G^*(\omega)| \propto \omega^{3/4}$. This effective power law, which is different from that predicted for flexible polymers but similar to that predicted for uncrosslinked semi-flexible polymers, results from the finite rigidity of actin filaments. We are currently studying the effect of actin concentration on the rheology of crosslinked actin networks.

Acknowledgments The Authors thank D. Morse and Scot C. Kuo for insightful conversations and T.G. Mason and K. Rufener for their help in the DWS measurements. We thank R.D. Mullins, J.F. Kellerher, and T.D. Pollard for their generous gift of *Acanthamoeba a*-actinin. This work was supported by the Whitaker Foundation and the National Science Foundation, grants DMR 9623972 (CAREER), CTS 9502810, and CTS 9625468.

Appendix

In this section, we establish a relationship between the mean square displacement of a microsphere imbedded in a viscoelastic fluid and the creep compliance of that fluid. The shear stress and shear strain are related to one another as

$$\tau(t) = - \int_0^t G_r(t-t') \dot{\gamma}(t') dt' \quad (A.1)$$

$$\gamma(t) = \int_0^t J(t-t') \dot{\tau}(t') dt' \quad (A.2)$$

where $\dot{\tau} = d\tau/dt$ and $\dot{\gamma} = d\gamma/dt$ are the rates of change of the shear stress and shear strain, $G_r(t)$ is the linear stress relaxation modulus, and $J(t)$ is the linear creep compliance. Physically, $G_r(t)$ is the stress generated by a step strain $\gamma = \gamma_0 H(t)$ where $H(t)$ is a Heaviside function and $J(t)$ is the strain resulting from a step of stress $\tau = \tau_0 H(t)$. For instance, in an elastic solid

$$G_r(t) = G_0 \text{ and } J(t) = \frac{1}{G_0} \quad (A.3)$$

For a purely viscous fluid of viscosity η ,

$$G_r(t) = \eta \delta(t) \text{ and } J(t) = \frac{t}{\eta} H(t) \quad (A.4)$$

Unilateral Laplace transformation of Eqs. (A.1) and (A.2) yields simple relationships between the transforms $\tilde{J}(s)$, $\tilde{G}(s)$, and $\tilde{\gamma}(s)$:

$$\tilde{\tau}(s) = s \tilde{G}(s) \tilde{\gamma}(s) = \tilde{G}(s) \tilde{\gamma}(s) \quad (A.5)$$

$$\tilde{\gamma}(s) = s \tilde{J}(s) \tilde{\tau}(s). \quad (A.6)$$

Hence,

$$s \tilde{J}(s) \tilde{G}(s) = 1, \quad (A.7)$$

which establishes a relation between the Laplace transforms of the creep compliance and of the stress relaxation modulus. Since $s \tilde{G}(s) \langle \Delta \tilde{r}^2(s) \rangle = k_B T / \pi a$ (see Eq. 1), we can directly relate $\langle \Delta \tilde{r}^2(s) \rangle$ to $\tilde{J}(s)$ as

$$\langle \Delta \tilde{r}^2(s) \rangle = \frac{k_B T}{\pi a} \tilde{J}(s)$$

or

$$\langle \Delta r^2(t) \rangle = \frac{k_B T}{\pi a} J(t) \quad (A.8)$$

using $J(0)=0$. Equation (A.8) is approximate because Eq. (1) has not been demonstrated rigorously. Also, Eq. (A.8) neglects inertial effects, which become important at time scales $t < 10^{-6}$ s. Equation (A.8) yields the correct results for the extreme cases of a purely viscous fluid and a purely elastic solid. For a viscous liquid, $\langle \Delta r^2(t) \rangle = 6DtH(t) = (k_B T / \pi \eta a) t H(t)$ and $J(t) = (t/\eta) H(t)$, which verifies Eq. (A.4). For an elastic solid, $\langle \Delta \tilde{r}^2(s) \rangle = r_0^2$ and $J(t) = 1/G_0$, where $G_0 = k_B T / \pi a r_0^2$, which verifies Eq. (A.3).

References

- Alberts B, Bray D, Lewis J, Rabb M, Roberts K, Watson J (1994) Molecular biology of the cell. 3rd Ed Garland Publishing
- Doi M, Edwards SF (1989) The theory of polymer dynamics. Clarendon Press, Oxford
- Ferry JD (1980) Viscoelastic properties of polymers. John Wiley and Sons, New York
- Gittes F, Mickey B, Nettleton J, Howard JJ (1993) Flexural rigidity of microtubules and actin filaments measured from thermal fluctuations in shape. *J Cell Biol* 120:923–934
- Gittes F, Schnurr B, Olmsted PD, Macintosh FC, Schmidt CF (1997) Microscopic viscoelasticity: shear moduli of soft materials determined from thermal fluctuations. *Phys Rev Lett* 79:3286–3289
- Isambert H, Venier P, Maggs AC, Fattoum A, Kassab R, Pantaloni D, Carlier MF (1995) Flexibility of actin filaments derived from thermal fluctuations. *J Biol Chem* 270:11437–11444
- MacLean-Fletcher SD, Pollard TD (1980) Viscometric analysis of the gelation of *acanthamoeba* extracts and purification of two gelation factors. *J Cell Biol* 85:414–428
- Mason TG, Weitz DA (1995) Optical measurements of frequency-dependent linear viscoelastic moduli of complex fluids. *Phys Rev Lett* 74:1252–1255
- Mason TG, Dhople A, Wirtz D (1997) Rheology and microrheology of concentrated DNA solutions. In: Wirtz D, Halsey TC (eds) *Statistical mechanics in physics and biology*. MRS Symp Proc 463:15–20
- Mason TG, Ganesan K, van Zanten J, Wirtz D, Kuo SC (1997) Particle-tracking microrheology of complex fluids. *Phys Rev Lett* 79:3282–3285
- Morse D (1997) preprint
- Rouse PE (1953) A theory of the linear viscoelastic properties of dilute solutions of coiling polymers. *J Chem Phys* 21:1272–1276
- Sato M, Schwarz WH, Pollard TD (1989) Dependence of the mechanical properties of actin/*a*-actinin gels on deformation rate. *Nature (London)* 325:828–830
- Schnurr B, Gittes F, Olmsted PD, Schmidt CF, Macintosh FC (1997) In: Wirtz D, Halsey TC (eds) *Local viscoelasticity of biopolymer solutions statistical mechanics in physics and biology*. MRS Symp Proc 463:15–20
- Spudich JA, Watt SJ (1971) The regulation of rabbit skeletal muscle contraction. *J Biol Chem* 246:4866–4871
- Tempel M, Isenberg G, Sackmann E (1996) Temperature-induced sol-gel transition and microgel formation in *a*-actinin cross-linked actin networks: a rheological study. *Phys Rev E* 54:1802–1808
- Wachstock D, Schwarz WH, Pollard TD (1993) Affinity of *a*-actinin for actin determines the structure and mechanical properties of actin filament gels. *Biophys J* 65:205–214
- Wachstock D, Schwarz WH, Pollard TD (1994) Crosslinker dynamics determine the mechanical properties of actin gels. *Biophys J* 66:801–809
- Weitz DA, Pine DJ (1993) In: Wyn B (ed) *Dynamic light scattering*. Oxford University Press, Oxford
- Wirtz et al. unpublished results
- Xu J, Wirtz D, Pollard TD (1998) The dynamics of crosslinking determine the rheological properties of actin filament networks. To appear in *J Biol Chem*
- Zimm BH (1956) Dynamics of polymer molecules in dilute solutions: Viscoelasticity, flow birefringence, and dielectric loss. *J Chem Phys* 37:2547–2568